# Identification and Prediction for the Long Range Runoff Systems

By

Tojiro Ishihara*, Takuma Takasao* and Shuichi Ikebuchi*

In this paper, the runoff simulation method has been discussed in order to obtain effective information for water resource planning. The framework consists of the identification of the long range runoff systems and the simulation for the areal daily precipitation while the runoff data are simulated by their combination.

First, for identifying the long range runoff systems, the improved statistical unit hydrograph method is proposed based on the techniques of information theory. Next, the daily precipitation data are simulated over a long period and in a wide area through the successive combination of regional correlation analysis between the base or sub-base and surrounding stations, spatial simulation between the base and sub-base stations, and sequential simulation at the base station. Finally, by the combination of the improved statistical unit hydrograph method and the simulation method for areal daily precipitation, the observed data are shown with sufficient accuracy.

## 1. Introduction

In the development of water resource planning and design, it is a basic problem to establish techniques for the long range runoff simulation. Most studies on runoff simulation are based on time series analysis of runoff data. Because of the short length of observed runoff data, however, the stability of frequency distribution is in itself a problem and moreover, it seems to be an essential defect that those methods pay no attention to the runoff mechanism. In addition to those circumstances, considering that long range runoff phenomena are essentially stochastic processes and the observed daily precipitation data are better in length and accuracy than runoff data, the runoff simulation should be constructed by the following procedures:

First, construct the basin system model from both the observed runoff data and corresponding precipitation data. In this case, we should introduce into the model
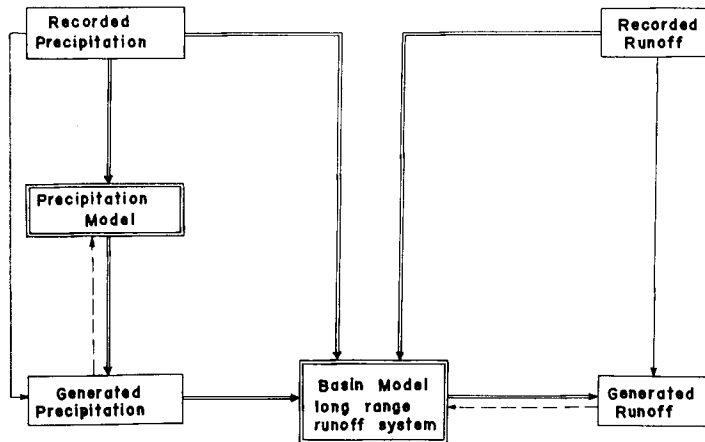
---

* Department of Civil Engineering

Fig. 1.   Flow chart for runoff simulation.

not only the deterministic or physical characteristics but also the statistical laws involved in the transformation system from precipitation to river discharge.

Next, complement the lack of runoff data from the combination of the basin model and observed daily precipitation data.   Furthermore, for predicting the future the daily river discharge, establish the simulation methods of daily precipitation in space and time and combine them with the basin system model.

Finally, it may be concluded that the runoff simulation consists of making the basin system model and establishing the simulation method of daily precipitation in space and time.   The flow chart for the above description is shown in Figure 1.

## 2.   Improved statistical unit-hydrograph method

The authors are interested in information theory, especially in Wiener's filtering theory and have investigated how to apply this theory to long range runoff systems[1].

At first, the statistical properties of daily precipitation and river discharge series are discussed by using correlation analysis.   Then, after the time-invariant-linearization of runoff system is made according to the physical mechanism of runoff phenomena, the unit-impulse response function is derived from the Wiener-Hopf equation.   We have designated this response as "the statistical unit-hydrograph", and subsequently written it as SUH.   The results applied to the Yura River basin have verified that the SUH method may be effective for identifying the long range runoff system.   At the same time, however, there still have remained some problems, such as the peak values of SUH differ from year to year and the accuracy of prediction is unsatisfactory, especially in the lower stages of river discharge.   These problems result from the fact

that separation method of surface runoff from observed hydrographs is still unsatisfactory and the subsurface and groundwater runoffs are considered as the same runoff system in spite of their different linearities.

From these circumstances, the authors hope to improve and modify the SUH method by the following approach: The major improvements and modifications are to divide the observed hydrographs into the subsurface and groundwater runoff components and to introduce the effect of evapotranspiration on water content in the subsurface stratum into the model.

## 2-1. Supplies to subsurface and groundwater runoff systems

The runoff process depends on time-distribution of water content in the subsurface stratum. In the rainy season, especially, we must remove the initial loss and the surface runoff components from observed daily precipitation data, for estimating the effective input data for linear system. Figure 2 shows a schematic representation of water content distribution in the subsurface stratum. In Fig. 2, *Ws, Wc* and *Wa* are the saturated water content, the capillary saturated water content and the adsorbed water content respectively. Each value is determined from the product of depth and effective porosity of subsurface stratum[2].
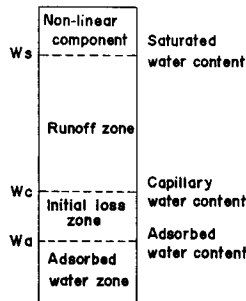


Fig. 2. Schematic representation of water content distribution in the subsurface stratum.

For the purpose of practical runoff analysis, we define the runoff zone as domain *Wc-Ws* and the initial loss zone as domain *Wa-Wc*. Furthermore, considering that surface runoff is proportional to water content in the subsurface stratum, we may find that water contents in the runoff zone and in the initial loss zone decrease according to Eqs. (1) and (2) respectively.

$$S(i+1) = \{S(i)+(f_c+e_v(i))/a\}\,e^{-a}-(f_c+e_v(i))/a \tag{1}$$

$$S(i+1) = S(i)-e_v(i) \tag{2}$$

in which $S(i)$ and $S(i+1)$ are water contents in the day $i$ and $i+1$, $a$, the recession coefficient of subsurface runoff, $f_c$, the final infiltration rate and $e_v(i)$, the daily evapotranspiration rate. Consequently, the daily decrease rate of water content in the runoff zone $DS(i)$ $(=S(i)-S(i+1))$, is divided into components $Rs(i)$ and $R_G(i)$, supplied to the subsurface and groundwater runoffs respectively. In this case, because the maximum value of input component to the groundwater runoff system equals $f_c$, it follows that:

$$
\left.
\begin{array}{l}
\left.
\begin{array}{l}
Rs(i) = DS(i) - (f_c + e_v(i)) \\
R_G(i) = f_c
\end{array}
\right\} \quad \text{if } DS(i) \geq f_c + e_v(i) \\[2mm]
\left.
\begin{array}{l}
Rs(i) = 0 \\
R_G(i) = DS(i) - e_v(i)
\end{array}
\right\} \quad \text{if } DS(i) < f_c + e_v(i)
\end{array}
\right\}
\qquad (3)
$$

When it rains, $S(i)$ being in the runoff zone, $(S(i)+R(i))$ corresponds to $S(i)$, in which $R(i)$ is daily precipitation intensity. Of course, this is true only if $Wc < S(i) + R(i) \leq Ws$. On the other hand, the initial loss component $L(i)$ and the surface runoff component $NL(i)$ are estimated as follows:

$$
\left.
\begin{array}{ll}
L(i) = Wc - S(i) & \text{if } S(i) + R(i) \geq Wc \\
L(i) = R(i) & \text{if } S(i) + R(i) < Wc \\
NL(i) = S(i) + R(i) - Wc & \text{if } S(i) + R(i) \geq Ws
\end{array}
\right\}
\qquad (4)
$$

Next, it is an important problem to estimate the daily evapotranspiration rate. Considering that the evapotranspiration rate $e_v(i)$, is highly correlated with the pan evaporation rate $E(i)$ and water content in the subsruface stratum $S(i)$, the relationship between $e_v(i)$, $E(i)$ and $S(i)$ may be expressed by Figure 3[3]. Therefore, in the runoff zone, $e_v(i)$ may be replaced by $E(i)$ and in the initial loss zone $e_v(i)$ may be replaced by Eq. (5).
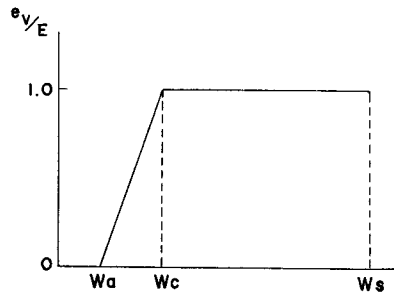


Fig. 3.  Relationship between soil moisture content and evapotranspiration.

$$e_v(i) = \{S(i) - Wa\} \cdot E(i)/(Wc - Wa) \tag{5}$$

Unfortunately, if pan evaporation has not been observed in the runoff zone, we must neglect $e_v(i)$ and estimate $e_v(i)$ with Eq. (6) in the initial loss zone.

$$S(i+1) = S(i) \cdot e^{-\beta} \tag{6}$$

in which $\beta$ is the recession coefficient of water content in the initial loss zone.

## 2-2. Prediction for the amount of groundwater runoff

Assuming that the groundwater runoff system is linear, we can predict the amount of groundwater runoff $Q_G^*(i)$ by the following equation, in which $h_G(\tau)$ is the unitgraph of groundwater runoff system and is given by Figure 4.

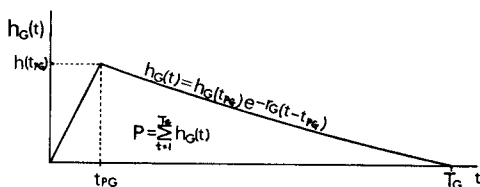$$Q_G^*(i) = \sum_{\tau=0}^{T_G} h_G(\tau) \cdot R_G(i-\tau) \tag{7}$$



Fig. 4. Unitgraph of groundwater runoff system.

In Fig. 4, $r_G$ is the recession coefficient of groundwater runoff (It is estimated from the observed hydrographs); $t_{PG}$, the peak lag time (in most cases, $t_{PG}$=one day): $T_G$, the duration time for the groundawter runoff over a long period of time ($T_G$=40–50 days is suitable for practical purposes); and p, the loss rate discharged into the deeper groundwater layer and other basins (In general, though, the value nearly equals 1.0 in the upper basin area, and is less than 1.0 in the downward. For practical analysis, when the hydrographs $Q_G^*(i)$ do not agree with observed groundwater hydrograph, the value p may be changed. This process is repeated until $Q_G^*(i)$ is judged to be an adequate representation of groundwater hydrograph).

## 2-3. Statistical unit hydrograph of subsurface runoff system

Separating the groundwater runoff estimated by Eq. (7) from the observed hydrographs and moreover, removing the surface runoff component from the residual hydrographs, we get the subsurface runoff hydrographs $Q_s(i)$. Then, we can find the statistical unit hydrograph of subsurface runoff system $h_s(\tau)$ from solving the following

Wiener-Hoph equation with $R_s(i)$ as input and $Q_s(i)$ as output[4]:

$$\Phi_{RQ}(\tau) = \sum_{k=0}^{Ts} h_s(k) \cdot \Phi_{RR}(\tau - k) \tag{8}$$

in which $\Phi_{RR}(\tau)$ and $\Phi_{RQ}(\tau)$ are given by Eqs. (9) and (10):

$$\Phi_{RR}(\tau) = \frac{1}{N-\tau} \sum_{i=1}^{N-\tau} Rs(i) \cdot Rs(i+\tau) \tag{9}$$

$$\Phi_{RQ}(\tau) = \frac{1}{N-\tau} \sum_{i=1}^{N-\tau} Rs(i) \cdot Qs(i+\tau) \tag{10}$$

where $N$ is the number of days for the period considered, and $Ts$ is a duration time of subsurface runoff.

In this case, provided the maximum value of subsurface runoff be approximated by the maximum daily decrease rate of water content in the runoff zone, the value $DSmax$ may be given as follows:

$$DSmax \fallingdotseq (Ws - Wc + fc/a)(1 - e^{-a}) - fc \tag{11}$$

Therefore, as first step, when the difference between $Q_G^*(i)$ and observed hydrograph $Q(i)$ is larger than $DSmax$, the excess part is separated as the surface runoff component, and the subsurface runoff $Q_s^*(i)$ may be predicted by the following equation:
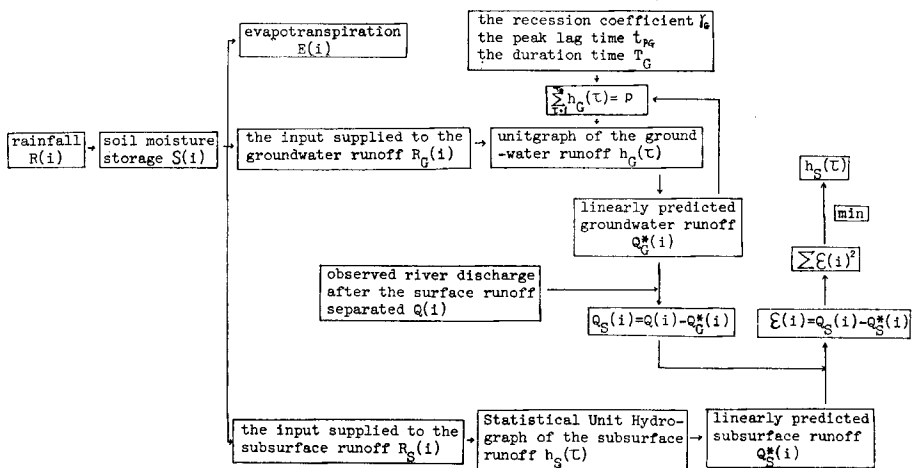


Fig. 5.   Flow chart for the improved statistical unit hydrograph method.

$$Q_s^*(i) = \sum_{\tau=0}^{T_s} h_s(\tau) \cdot R_s(i-\tau) \tag{12}$$

However, considering that the maximum value DSmax does not discharge into the subsurface runoff in a moment, the separation of surface runoff component should be practically modified by the following approach. That is to say, only when $Q_s^*(i)$ predicted by Eq. (12) is smaller than $Qs(i)$ under the condition of $Rs(i-1)=$DSmax or $\approx$ DSmax, the difference between $Q_s^*(i)$ and $Qs(i)$ should be separated as surface runoff component, namely $Qs(i)=Q_s^*(i)$, and in other days, $Qs(i)=Q(i)-Q_s^*(i)$. Ultimately, the SUH of subsurface runoff system may be estimated between such modified $Qs(i)$ and $Rs(i)$. The flow chart of the above procedures is shown in Figure 5.

## 3. Stochastic structures in space and time of daily precipitation and their simulation

### 3-1. Classification of precipitation stations

Though there are many stations for acquiring precipitation data, we have experienced situations when usable records are sparse, unavailable, or quite short in the time length of observation. In other situations, precipitation records may be adequate in length and accuracy, but quite sparsely distributed areally. Thus, it becomes increasingly important to estimate the precipitation variables at a number of observing stations for relatively short periods of time from observations taken at one station over a long interval of time.

In this paper, we classify observing stations into the base station, the sub-base stations and the surrounding stations, and estimate the stochastic structures in space and time from their interrelations and lastly, simulate the daily precipitation sequences. Where the base station is a representative station in the basin and adequate both in length and accuracy; the sub-base station is a representative station in the tributary and shorter in length than the base station; and the last stations are surrounding the base and sub-base stations and are inadequate in length and accuracy.

### 3-2. Regional correlation analysis between the base or the sub-base station and the surrounding stations

The statistical concepts of correlation analysis play an important role to interpolate the precipitation variable. The inter-station correlation coefficient $r$ equals:

$$r = \frac{\sum\limits_{i=1}^{n} x_i y_i - n \cdot \bar{x} \cdot \bar{y}}{\sqrt{\left(\sum\limits_{i=1}^{n} x_i^2 - n \cdot \bar{x}^2\right)\left(\sum\limits_{i=1}^{n} y_i^2 - n \cdot \bar{y}^2\right)}} \tag{13}$$

and is a measure of association between the variables, $x_i$ and $y_i$, taken simultaneously in time at the base and the surrounding stations, provided linear association between $x_i$ and $y_i$, $y_i$ will be predicted as follows:

$$y_i = \hat{a} \cdot x_i + \hat{\beta} + \varepsilon_i \tag{14}$$

in which $\hat{a}$ and $\hat{\beta}$ are given by Eq. (15) and $\varepsilon$ is the residual random variable.

$$\left.\begin{aligned} \hat{a} &= r \cdot \sqrt{\frac{\left(\sum\limits_{i=1}^{n} y_i^2 - n \cdot \bar{y}^2\right)}{\left(\sum\limits_{i=1}^{n} x_i^2 - n \cdot \bar{x}^2\right)}} \\ \hat{\beta} &= \bar{y} - \hat{a} \cdot \bar{x} \end{aligned}\right\} \tag{15}$$

However, considering that the pairs of daily precipitation $(x_i, y_i)$ have generally bivariate exponential distribution, we must modify the above procedures as follows: Between higher correlated stations, we have experienced that the residual random variable $\varepsilon$ distributes normally within the subdivided classes of $x$. Thus, we estimate the standard deviation $\sigma_\varepsilon$ in each subdivision of the residual series $\{y_i - (\hat{a} \cdot x_i + \hat{\beta})\}$ and generate $\varepsilon_i$ according to the class of $x$, based on standard normal distribution $N(0, \sigma_\varepsilon)$. In the end, we can relate $y_i$ to $x_i$ and estimate missing data as accurately as feasible by Eq. (14).

Furthermore, combining the surrounding stations so that the regional correlations on the base station are the same, we can describe isolines of inter-station correlation coefficient about a base station[5]. Because the correlation between variables at different points tend to decrease with an increase of distance and difference in height between points, isolines do not show concentricity.

### 3-3. Spatial simulation between the base and sub-base stations

Because the great increase of distance between the base and sub-base stations makes the regional correlation coefficient lower, it is difficult to apply directly the above procedure to the correlation analysis between both points. Thus, we define four systems from the precipitation and no precipitation states of the base and sub-base stations: First; precipitation-precipitation system $(R.R)$, second; precipitation-no precipitation system $(R.D)$, third; no precipitation-precipitation system $(D.R)$, fourth;
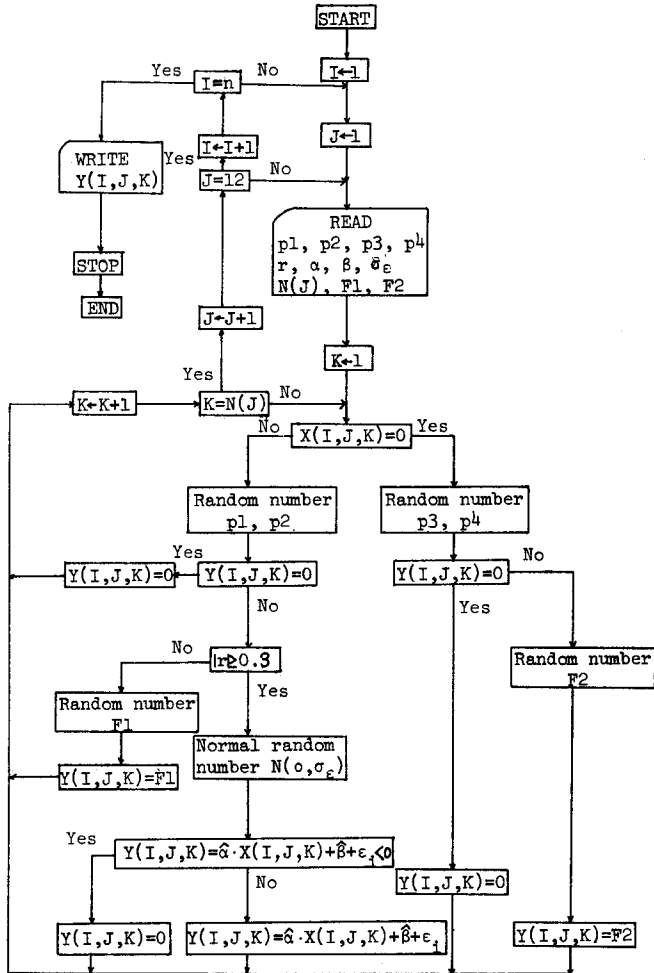
Fig. 6. Flow chart for the spatial simulation between the base and sub-base stations.

no precipitation-no precipitation system ($D.D$). Table 1 shows their occurrence probabilities.

Also, we have observed that the sub-base stations have themselves inherent occurrence probabilities. In general, the values $P_2$ and $P_3$ are higher with an increase

Table 1.　Occurrence probabilities of (R.R), (R.D), (D.R) and (D.D) systems.

| Base station \ Sub-base station | R | D | |
|---|---|---|---|
| R | P1 | P2 | P1+P2 = 1 |
| D | P3 | P4 | P3+P4 = 1 |

of distance and difference of height between the base and sub-base stations, and the value $P_1$ in rainy and typhoon seasons is higher compared with any other season.

Next, in $(R.R)$ and $(D.R)$ systems, we must estimate the daily precipitation at the sub-base station.　For $(R.R)$ system, the daily precipitation $R(i)$ at sub-base station will be estimated by the same equation as Eq. (14).　In this case, if $|r|<0.3$, the daily precipitation will be generated independently from the distribution of daily precipitation at sub-base station, $F_1$.　For $(D.R)$ system, the daily precipitation will be generated independently from the distribution of daily precipitation at sub-base station, $F_2$.　Where $F_1$ and $F_2$ are estimated from samples contained in $(R.R)$ and $(D.R)$ systems respectively.

Figure 6 shows the flow chart for the above procedures on spatial simulation.

## 3-4.　Sequential simulation at the base station

It still remains to simulate the daily precipitation at the base station for predicting future precipitation over a long period.

We consider two processes $(R^*(i'), D(i'))$ $(i'=1, 2,\text{----})$ instead of one single process of the daily precipitation $R(i)$ $(i=1, 2,\text{----})$.　Figure 7 shows two processes of daily precipitation.　In Fig. 7, $R^*(i')$ corresponds to the precipitation intensity $R(i)>0$, and $D(i')$ corresponds to the continuous dry days.

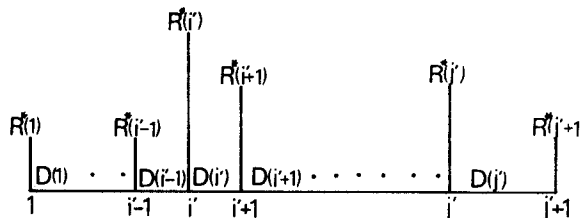Next, assumed that 1) these vectors are mutually independent and have a common



Fig. 7.　Illustration of the daily precipitation intensity R*(i) and the continuous dry days D(i).

distribution function, and 2) $R^*(i')$ is independent of $D(i')$, we may transform the daily precipitation $R(i)$ into two mutually independent processes, $(R^*(i'), D(i'))$.

Therefore, we may simulate the daily precipitation at the base station by the following procedures:

1) For each month, count the frequency distributions of $R^*$ and $D$ respectively.
2) For each $R^*$ and $D$, divide up the year into the months with similar distribution by the $\chi^2$-test of independence.
3) Reorganize the months with similar distribution for both $R^*$ and $D$, and call those months "populations".
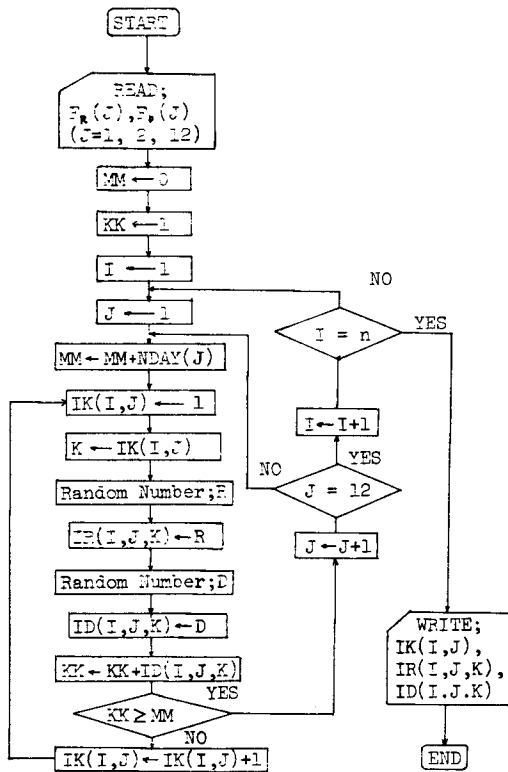


I; Year       $F_R(J)$; Distribution function of
J; Month            the daily precipitation intensity
KK; Day       $F_p(J)$; Distribution function of
MM; Total days       the continuous dry days
  n; Simulated year    IR(I,J,K); Simulated precipitation intensity
NDAY(J); Days of J-th month   ID(I,J,K); Simulated dry days
IK(I,J); Number of precipitation days

Fig. 8. Flow chart for the sequential simulation at the base station.

4) For each population, after the probabilities of exceedance over the subdivided classes are calculated for $R^*$ and $D$, the distribution functions $F_R$ and $F_D$ are estimated from the least square method.

Once the populations are defined and the functions $F_R$ and $F_D$ are determined, the daily precipitation may be simulated according to Figure 8.

## 4. Application to the Yodo River basin and their results

### 4-1. The research data

Figure 9 shows the general map of the basin.   The basin may be divided broadly

Gaging station of stage

a. Yasu
b. Mikumo
c. Ugawa
d. Toriigawa
e. Kurotzu
f. Yodo
g. Kameoka
h. Nhoso
i. Shimagahara
j. Nabari
k. Kamo
l. Hirakata

Rain gage station

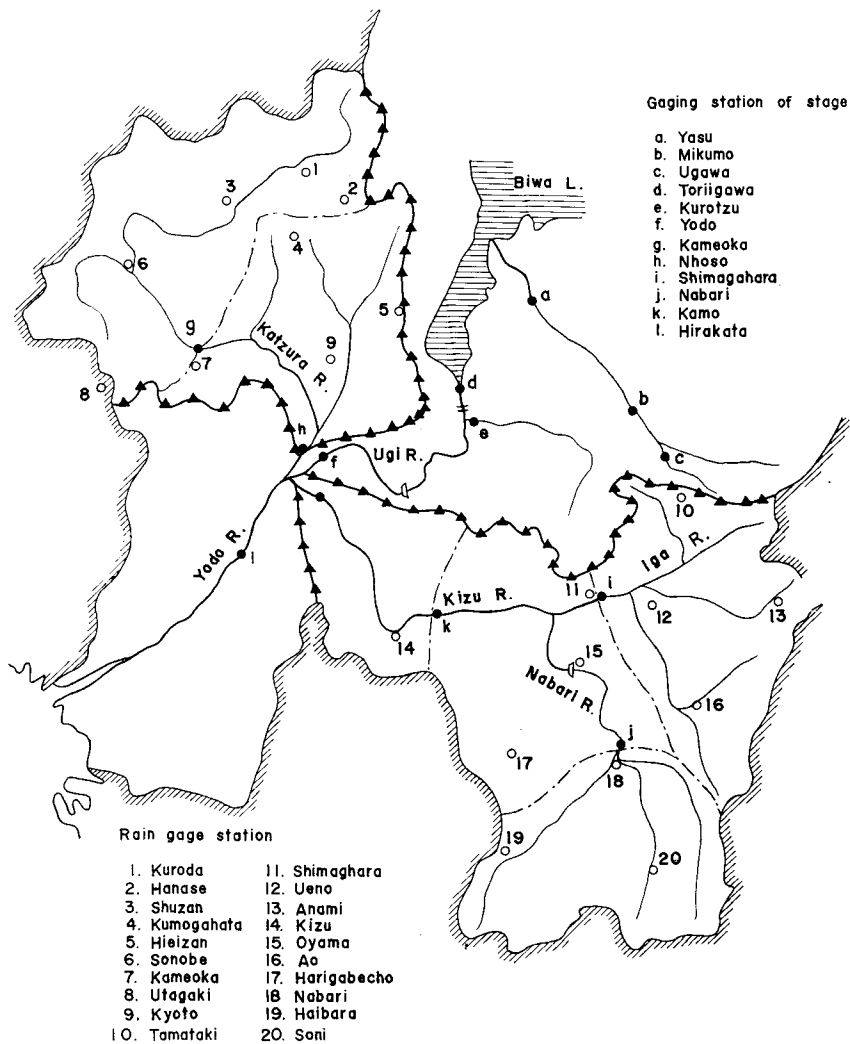| | |
|---|---|
| 1. Kuroda | 11. Shimaghara |
| 2. Hanase | 12. Ueno |
| 3. Shuzan | 13. Anami |
| 4. Kumogahata | 14. Kizu |
| 5. Hieizan | 15. Oyama |
| 6. Sonobe | 16. Ao |
| 7. Kameoka | 17. Harigabecho |
| 8. Utagaki | 18. Nabari |
| 9. Kyoto | 19. Haibara |
| 10. Tamataki | 20. Soni |

Fig. 9.   General map of Yodo River basin.

into Kizu, Uji and Katsura River basins and in the upper region of Uji River basin there is Lake Biwa. The research data for identifying the long range runoff systems are Kameoka and Nohso in the Katsura River basin, and Nabari, Shimagahara and Kamo in the Kizu River basin. Because of the storage effect by Lake Biwa and an artifical control by Amagase dam, the Uji River basin was not analyzed.

Furthermore, the areal precipitation as input data to those analytical basins was calculated by the Thiessen method of precipitation stations shown in Fig. 9.

## 4-2. Unitgraph of groundwater runoff system and SUH of subsurface runoff systems

Once the daily decrease rate of water content in the subsurface stratum was calculated according to Eqs. (1) and (2), the unitgraph of groundwater runoff system and the SUH of subsurface runoff system are estimated based on Fig. 5. The analytical constants and parameters are summarized in Table 2. The runoff rate p in the downstream becomes smaller than that in the upstream.

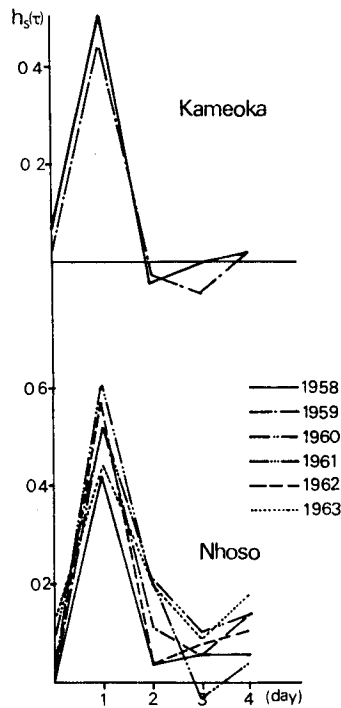Also, Fig. 10 shows the improved statistical unit hydrograph of subsurface runoff



Fig. 10. Statistical unit hydrograph of subsurface runoff system at Kameoka and Nohso stations.

Table 2. Analytical constants and parameters.

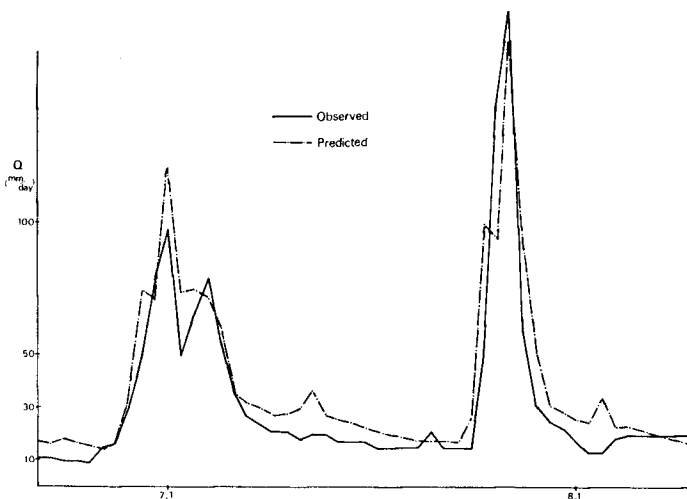| Watershed | $\alpha$ (hr$^{-1}$) | $t_2$-$t_1$ (hr) | $\gamma D$ (mm) | $\beta$ (day$^{-1}$) | $r_G$ (day$^{-1}$) | $T_G$ (day) | $t_{PG}$ (day) | p* |
|-----------|------|------|-----|-------|--------|----|----|-----|
| Kameoka | 0.0245 | 100 | 110 | 0.026 | 0.0700 | 50 | 1 | 1.0 |
| Nhoso | 0.0339 | 80 | 110 | 0.026 | 0.0550 | 50 | 1 | 0.9 |



Fig. 11. Comparison between the observed and predicted river discharges at Kameoka.

system at Kameoka and Nohso. They coincide very well every year, not only in the whole shape but also in their peak values. Furthermore, the sum of predicted sub-surface runoff and groundwater runoff components is shown in Fig. 11 compared with the observed runoff sequences. They coincide very well and it may be concluded that the prediction of groundwater and subsurface runoff is very satisfactory.

## 4-3. Spatial and sequential simulation results on the daily precipitation

For simulating the daily precipitation, Kyoto station was selected as the base station and Sonobe and Ueno stations as the sub-base stations. Their data length are 80 years (1886–1965) at Kyoto, 40 years (1926–1965) at Sonobe, 28 years (1938–1965) at Ueno and 6 years (1958–1963) at other stations. Fig. 12 shows the isolines of inter-station correlations about Kyoto, Sonobe and Ueno stations.

Table 3 shows the occurrence numbers of $(R.R)$, $(R.D)$, $(D.R)$ and $(D.D)$ systems between Ueno, Sonobe and Kyoto stations. The occurrence number of $(R.R)$ system is smaller than that of $(D.D)$ system. On the other hand, though the number of $(R.D)$ nearly equals that of $(D.R)$ throughout the year between Kyoto and Ueno, for Sonobe

station, $(D.R)$ system has a great occurrence number in winter season. Also, Table 4 shows the comparison between observed data and simulated data with different standard deviations for $R^*(i) \geq 10$ and $R^*(i) < 10$ (mm/day). The simulated data has

Table 3. Occurrence numbers of (R.R), (R.D), (D.R) and (D.D).

| MONTH / STATION | 1 | | 2 | | 3 | | 4 | | 5 | | 6 | |
|---|---|---|---|---|---|---|---|---|---|---|---|---|
| OSAKA (1926–1945) | 92 | 53 | 108 | 54 | 164 | 74 | 168 | 43 | 168 | 35 | 183 | 42 |
| | 26 | 447 | 23 | 373 | 37 | 343 | 29 | 358 | 28 | 387 | 39 | 334 |
| UENO (1938–1945) | 31 | 19 | 54 | 9 | 82 | 13 | 69 | 10 | 76 | 4 | 87 | 10 |
| | 13 | 183 | 20 | 139 | 14 | 137 | 12 | 147 | 13 | 153 | 13 | 128 |
| HIKONE (1926–1945) | 116 | 29 | 128 | 34 | 174 | 64 | 153 | 58 | 138 | 65 | 151 | 74 |
| | 220 | 253 | 158 | 238 | 104 | 276 | 73 | 314 | 59 | 356 | 65 | 308 |
| SONOBE (1926–1945) | 95 | 50 | 114 | 48 | 153 | 85 | 152 | 59 | 133 | 70 | 157 | 68 |
| | 108 | 365 | 100 | 296 | 88 | 292 | 76 | 311 | 64 | 351 | 76 | 297 |
| MONTH / STATION | 7 | | 8 | | 9 | | 10 | | 11 | | 12 | |
| OSAKA (1926–1945) | 160 | 89 | 131 | 76 | 185 | 38 | 159 | 33 | 133 | 39 | 102 | 52 |
| | 33 | 336 | 53 | 358 | 62 | 313 | 27 | 399 | 30 | 296 | 38 | 426 |
| UENO (1938–1945) | 70 | 23 | 64 | 19 | 73 | 21 | 73 | 8 | 53 | 11 | 36 | 15 |
| | 14 | 139 | 37 | 126 | 20 | 124 | 11 | 154 | 13 | 161 | 12 | 183 |
| HIKONE (1926–1945) | 164 | 85 | 125 | 82 | 179 | 68 | 143 | 49 | 123 | 49 | 102 | 52 |
| | 72 | 297 | 73 | 338 | 72 | 279 | 89 | 337 | 106 | 320 | 169 | 295 |
| SONOBE (1926–1945) | 175 | 74 | 131 | 76 | 184 | 63 | 133 | 59 | 123 | 49 | 103 | 51 |
| | 61 | 308 | 64 | 347 | 79 | 272 | 83 | 343 | 95 | 331 | 101 | 363 |

Table 4. Comparison between observed data and simulated data at Ueno.

| Month | 1 | 2 | 3 | 4 | 5 | 6 | 7 | 8 | 9 | 10 | 11 | 12 |
|---|---|---|---|---|---|---|---|---|---|---|---|---|
| R. R | 0.791 | 0.739 | 0.789 | 0.837 | 0.851 | 0.858 | 0.798 | 0.717 | 0.767 | 0.866 | 0.788 | 0.742 |
| | 0.656 | 0.757 | 0.731 | 0.738 | 0.864 | 0.679 | 0.611 | 0.641 | 0.655 | 0.727 | 0.756 | 0.651 |
| D. R | 0.081 | 0.093 | 0.114 | 0.082 | 0.109 | 0.142 | 0.171 | 0.186 | 0.142 | 0.102 | 0.076 | 0.104 |
| | 0.077 | 0.135 | 0.093 | 0.080 | 0.072 | 0.084 | 0.108 | 0.233 | 0.145 | 0.063 | 0.072 | 0.065 |

upper: observed    under: simulated
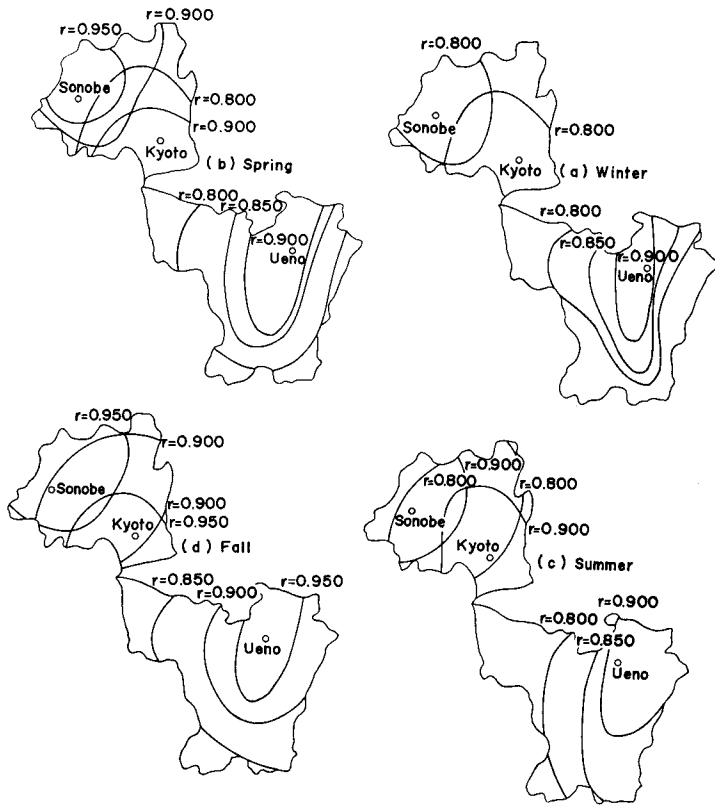
Fig. 12.   Isolines of inter-station correlations about Kyoto, Sonobe and
            Ueno stations.

good agreement with the observed, except for June and July.   We believe that if the
variable $R^*(i)$ are subdivided much more, their agreement will become better.
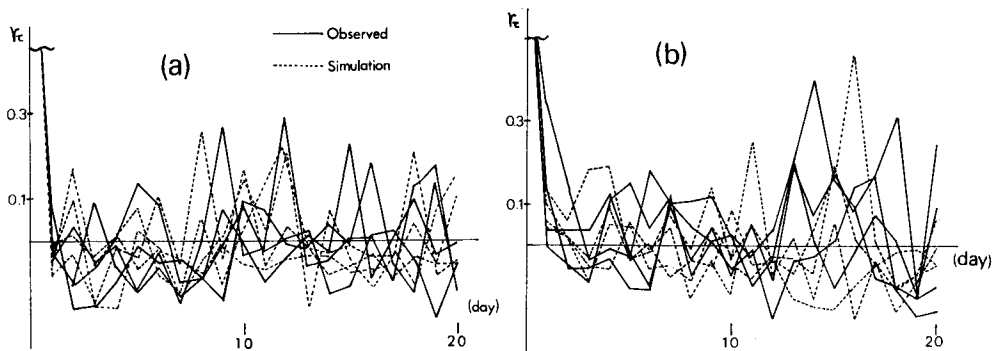


Fig. 13.   Comparison between observed and simulated data (daily precipitation)
            (a) Winter (b) Summer.

Table 5. Distributions of the daily precipitation intensity and the continuous dry days.

| Month | | 1 | 2 | 3 | 4 | 5 | 6 |
|---|---|---|---|---|---|---|---|
| Number of Precipitation days | Mean Value | 8.675 | 9.225 | 12.075 | 11.950 | 11.100 | 13.600 |
| | Variance | 11.815 | 7.461 | 8.994 | 7.741 | 5.733 | 12.810 |
| Number of Continuous dry days | Mean Value | 3.055 | 2.809 | 2.372 | 2.352 | 2.681 | 2.052 |
| | Standard Deviation | 3.025 | 2.527 | 1.937 | 1.806 | 2.369 | 1.820 |
| Month days divided by Mean value of Continuous dry days | | 9.820 | 9.968 | 12.647 | 12.755 | 11.189 | 14.619 |
| Month | | 7 | 8 | 9 | 10 | 11 | 12 |
| Number of Precipitation days | Mean Value | 12.525 | 9.825 | 12.650 | 9.700 | 8.350 | 8.050 |
| | Variance | 16.102 | 11.635 | 12.079 | 8.677 | 3.772 | 8.818 |
| Number of Continuous dry days | Mean Value | 2.275 | 2.776 | 2.178 | 2.813 | 3.361 | 3.326 |
| | Standard Deviation | 2.386 | 2.868 | 2.004 | 2.598 | 2.915 | 3.189 |
| Month days divided by Mean value of Continuous dry days | | 13.186 | 10.806 | 13.774 | 10.664 | 8.925 | 9.019 |

Finally, let us discuss the simulated results at Kyoto base station. Table 5 shows that the continuous dry days have approximately an exponential distribution and the number of precipitation days the poisson distribution respectively. Also, considering that the values at the lowest low nearly equals the mean value of the number of precipitation days, our treatment for two processes $R^*$ and $D$ may be effective for sequential simulation. Thus, we divided the year into the following seven populations by the $\chi^2$-test of independence. I, Dec., Jan., Feb.; II, Mar.; III, Apr., May; IV, Jun.,
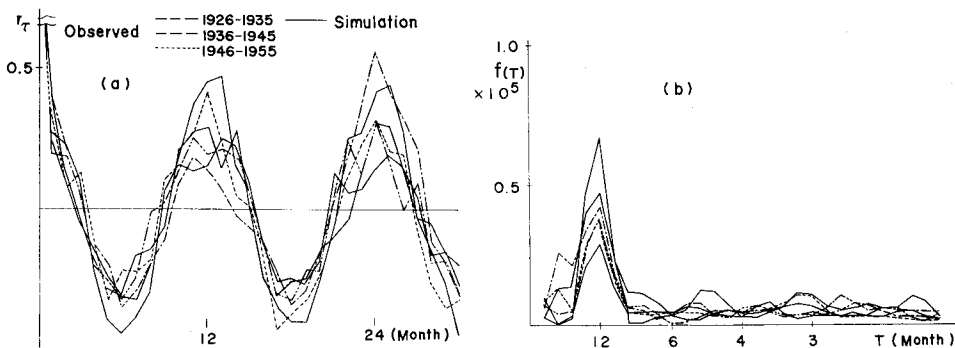


Fig. 14. Comparison between observed and simulated data (monthly precipitation)
(a) Correlogram (b) Power spectrum.

Jul.; V, Aug.; VI, Sep.; VII, Oct., Nov.. The comparisons between observed and simulated data are shown in Fig. 13 and Fig. 14. Fig. 13 corresponds to the daily precipitation and Fig. 14 to the monthly precipitation with the sum of simulated daily data. The simulated data reflects sufficiently the characteristics of observed data.

From the above results, we may conclude that methods proposed in this paper are effective for simulating the daily precipitation over a long period and in a wide area.

## 5.  Application to the runoff simulation at Nohso

### 5-1.  Areal precipitation as input to SUH method

Combining the simulated daily precipitation with the improved statistical unit hydrograph, we obtain the simulated runoff data. In this case, because the input to SUH are lumped data, we must estimate the areal precipitation from the simulated data given in section 4. The procedures are as follows:

a) for estimating the daily precipitation at all other stations up to the length of observed data at the sub-base station - First, determine the influential domain of the base or sub-base station from the regional correlation analysis between the base or sub-base station and the surrounding stations. Second, interpolate the daily precipitation at stations in the domain by Eq. (14). Lastly, these estimated data and the observed daily precipitation at the base or sub-base station are transformed into the areal daily precipitation by Thiessen method.

b) for estimating the daily precipitation at all other stations up to the length of observed data at the base station - In this case, interpolate the daily precipitation at the sub-base station with spatial simulation method between the base and sub-base stations. Next, using the regional correlation analysis, estimate the daily precipitation at all stations up to the length of observed data at the base station. The last procedure is the same as method a).

c) for estimating the daily precipitation at all other stations up to more than the length of observed data at the base station - Simulate the daily precipitation at the base station for long period with sequential simulation and using successively methods b) and a). The daily precipitation at all other stations are estimated up to more than the length of observed data at the base station. Lastly, combining these simulated data with the Thiessen method, we obtain the areal daily precipitation for a long period.

### 5-2.  Comparison between the observed and simulated runoff data

At Nohso in the Katsura River basin, the daily areal precipitation was simulated according to method b) in the previous section, 5-1. That is to say, once the influential domains of Kyoto base station and Sonobe sub-base station were determined from the

regional correlation results such as Fig. 12, and the daily precipitation at Sonobe was estimated from spatial simulation between Kyoto and Sonobe stations, we transformed the simulated data at the sub-base station and the observed data at the base station into the data at all other stations in their domains.　Finally, all of this data was transformed into the areal precipitation with the Thiessen method.

On the other hand, as for the basin system models, we used the average of the improved statistical unit hydrographs shown in Fig. 10 and the unitgraph with the same parameters as Table 2.　Therefore, combining the simulated daily areal precipitation with the long range runoff system models, the runoff data were simulated.

Fig. 15 shows the comparison between the observed and simulated data.　The simulated runoff data reflect sufficiently the observed data.　If we are allowed to hope for better agreement, we must improve the simulation method only in those days which show the greatest precipitation intensity.　However, considering that these methods are applied to June with intensive variation of river discharge, the good agreement between the observed and simulated data may verify that the combination of the improved statistical unit hydrograph method and the simulation method of the areal daily precipitation are effective for the runoff simulation.
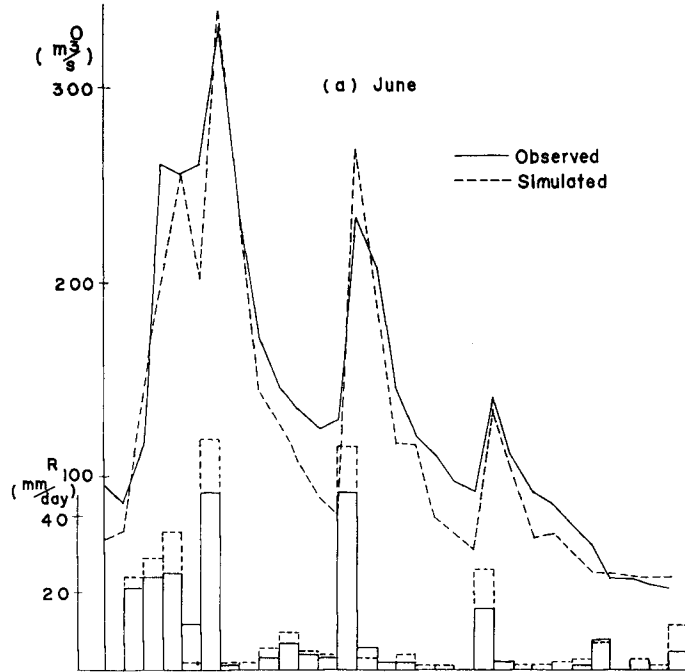
Fig. 15.　Comparison between observed and simulated data (areal daily precipitation and daily river discharge).

## 6. Conclusions

In this paper, the runoff simulation method has been discussed in order to obtain effective information for water resources planning. The framework consists of the identification of the long range runoff system and the simulation for the areal daily precipitations while the runoff data are simulated by their combination. The results obtained are summarized as follows:

1) The improved statistical unit hydrograph method is an effective method for the analysis and synthesis of long range runoff system responses, especially, the satisfactory agreement between the observed data and the predicted ones makes it possible to predict the daily runoff data and to complement the lack of runoff data.

2) Once the precipitation stations are classified into the base, sub-base and surrounding stations, the daily precipitation data are simulated over a long period and in a wide area through the successive combination of regional correlation analysis between the base or sub-base and surrounding stations, spatial simulation between the base and sub-base stations, and sequential simulation at the base station.

3) The simulated runoff data by the combination of SUH method and the simulation method for daily precipitation, reflect the observed data with sufficient accuracy. So, it is concluded that a series of these simulation techniques may offer useful information for water resources planning.

In the future, those methods will be applied to many other basins and techniques for water resources planning will be developed using these approaches.

### References

1) T. Takasao and S. Ikebuchi: A study of Long Range Runoff System Based on Information Theory, Dis. Prev. Res. Inst., Kyoto Univ. Annuals No. 12, 1969. (in Japanese)

2) T. Ishihara, Y. Ishihara, T. Takasao and C. Rai: A Study on the Runoff Characteristics of Yura River Basin, Dis. Prev. Res. Inst., Kyoto Univ. Annuals, No. 5, 1962. (in Japanese)

3) M. Kadoya: Analysis of Groundwater Flow in Small Mountain-Stream (1), Dis. Prev. Res. Inst., Kyoto Univ. Annuals No. 9, 1966 (in Japanese)

4) N. Wiener: Extraporation, Interporation and Smoothing of Stationary Time Series, John, Wiley, New York. 1949.

5) J. E. Caffey: Inter-Station Correlations in Annual Precipitation and in Annual Effective Precipitation, Colorado State Univ., 1965.